J. Nonlinear Sci. Vol. 11: pp. 279–304 (2001)
DOI: 10.1007/s00332-001-0397-5

Journal of
Nonlinear
Science

© 2001 Springer-Verlag New York Inc.

Squeeze Flow of Multiply-Connected Fluid Domains in a Hele-Shaw Cell

D. Crowdy and H. Kang
Department of Mathematics, Imperial College of Science, Technology and Medicine,
180 Queen's Gate, London, SW7 2BZ, U. K.
e-mail: d.crowdy@ic.ac.uk

Received September 20, 2000; accepted September 10, 2001
Online publication November 5, 2001
Communicated by M. Shelley

Summary. The theory of algebraic curves and quadrature domains is used to construct exact solutions to the problem of the squeeze flow of multiply-connected fluid domains in a Hele-Shaw cell. The solutions are exact in that they can be written down in terms of a finite set of time-evolving parameters. The method is very general and applies to fluid domains of any finite connectivity. By way of example, the evolution of fluid domains with two and four air holes are calculated explicitly. For simply connected domains, the squeeze flow problem is well posed. In contrast, the squeeze flow problem for a multiply connected domain is not necessarily well-posed and solutions can break down in finite time by the formation of cusps on the boundaries of the enclosed air holes.

1. Introduction

Shelley, Tian, and Wlodarski [18] have analysed the problem of a simply connected region of fluid evolving in a Hele-Shaw cell in which the two plates making up the cell move together or apart at some externally specified rate. Some exact analytical solutions of this problem are presented in [18] in the case where there are no regularization effects (such as surface tension). Most of these solutions pertain to the case of simply-connected fluid domains, but a solution for a doubly-connected fluid domain containing a single air hole is also given. This doubly-connected solution is the geometrically trivial case consisting of a time-evolving concentric annular domain. Results are also obtained in [18] concerning the existence, regularity, and uniqueness of solutions to the model problem of Hele-Shaw flow in a time-dependent gap. In particular, it is shown that the squeeze-flow initial value problem of a simply connected domain is well-posed and that an analytic interface at $t = 0$ remains analytic for $t > 0$. Physically, as the plates are squeezed together, the fluid spreads out and any incipient cusps are smoothed out.

Now consider the same squeeze flow problem in the case of a *multiply connected* domain in which a blob of fluid might contain a finite number of enclosed air holes. It is no longer obvious that in this problem the fluid boundaries will remain analytic for times $t > 0$ if they are analytic initially. In particular, this might reasonably be expected to depend on physical conditions imposed inside the enclosed air holes.

In the case of a simply connected blob, the question of the breakdown of solutions can be tackled analytically to a large extent because it has been found that a wide class of exact solutions exist [18]. The case of multiply-connected fluid regions is more complicated. Apart from the geometrically-trivial (doubly connected) concentric annulus solution [18], no other exact solutions for multiply connected domains evolving in squeeze flow are known, although it must be pointed out that, using elliptic function conformal maps, Varchenko and Etingof [21] and Richardson [13] [14] have identified exact solutions for the evolution of doubly-connected fluid domains in the physically distinct, but mathematically related, problem of *singularity-driven* Hele-Shaw flows, and many of those results can be adapted to the squeeze flow scenario.

In this paper, we present a new analytical method, based on exact solutions, for calculating the evolution of general multiply-connected fluid domains in the squeeze flow problem. It will be shown that the problem admits exact solutions in the sense that they can be written down, for times $t > 0$ (and for as long as they exist), in terms of a finite set of time-evolving parameters. The novelty of the method lies in our approach. Traditionally, exact solutions to free boundary problems of Hele-Shaw type are calculated by tracking the evolution of parameters appearing in a conformal map. In the case of simply connected domains, these parameters are the poles and zeros of a rational function (e.g. [11] [9] [12]); for doubly connected domains, they are the poles, zeros, and periods of an elliptic function [21] [13]. Here it is shown that exact solutions can be calculated equally well by tracking the evolution of a different (finite) set of parameters through exploitation of the fact that the boundaries of quadrature domains are algebraic curves.

The layout of the paper is as follows. In Section 2, it is shown that the dynamics of squeeze flow is such as to preserve quadrature domains. In Sections 3–5, the relevant theory of quadrature domains and algebraic curves is presented. In Section 6, a didactic example involving a doubly-connected fluid region is presented that allows a direct comparison of the new method with the traditional approach involving conformal mappings. Finally, by way of example, we present new classes of exact solution involving a triply connected domain with two air holes and a quintuply connected domain with four air holes.

2. Squeeze Flow in a Hele-Shaw Cell

Consider the evolution of a bounded N-connected fluid region $D(t)$ in a planar Hele-Shaw cell. Let $\partial D(t)$ denote the entire boundary of $D(t)$, which consists of disjoint components $\partial D_1(t)$—the outermost interface of the finite blob of fluid—and $\partial D_i(t)$, $i = 2, \ldots, N$—the $N-1$ closed interfaces bounding the $N-1$ enclosed holes contained within $\partial D_1(t)$.

Following [18], consider a model of the squeeze flow system given by

$$\mathbf{u}(x, y, t) = -\frac{b(t)^2}{12\mu}\nabla p(x, y, t), \qquad \text{in } D(t), \tag{1}$$

with

$$\nabla.\mathbf{u} = -\frac{\dot{b}(t)}{b(t)}, \qquad \text{in } D(t), \tag{2}$$

where $b(t)$ is the time-dependent gap width between the moving plates of the Hele-Shaw cell, μ is the fluid viscosity, and $\mathbf{u}$ denotes the two-dimensional gap-averaged fluid velocity. $p(x, y, t)$ denotes the pressure in the fluid. The dynamical boundary conditions are that

$$p = p_i(t), \qquad \text{on} \quad \partial D_i(t), \qquad i = 1 \ldots N, \tag{3}$$

where $p_i(t)$ is some (spatially constant) pressure inside the (disjoint) regions exterior to the fluid domain. Without loss of generality, one of these—$p_1(t)$, say—can be set equal to zero. A kinematic condition that each boundary of the domain moves with the fluid gives

$$\mathbf{u}.\mathbf{n} = V_n^i, \qquad \text{on} \quad \partial D_i(t), \qquad i = 1 \ldots N, \tag{4}$$

where V_n^i denotes the normal velocity of the boundary $\partial D_i(t)$.

The only differences between the above formulation and that of [18] are that the fluid domain is now multiply connected and that, in each hole, we are free to externally specify a pressure $p_i(t)$.

Define the velocity potential function

$$\phi \equiv -\frac{b(t)^2}{12\mu}p, \tag{5}$$

and define

$$4B(t) \equiv -\frac{\dot{b}(t)}{b(t)}; \tag{6}$$

then (1) and (2) imply that

$$\nabla^2\phi = 4B(t), \qquad \text{in } D(t), \tag{7}$$

and that, on $\partial D_i(t)$,

$$\begin{aligned} \phi &= a_i(t), \\ \nabla\phi.\mathbf{n} &= V_n^i, \end{aligned} \tag{8}$$

where

$$a_i(t) \equiv -\frac{b(t)^2}{12\mu}p_i(t). \tag{9}$$

In the next section, we define the notion of a *quadrature domain* and a *quadrature identity*. In order to see the relevance of the theory of quadrature domains to this physical problem, we prove the following theorem, which provides a result on the evolution of *quadrature identities*:

Theorem 2.1. *Under the dynamics of squeeze flow in a Hele-Shaw cell* (*as in the mathematical model just described*),

$$\frac{d}{dt}\int\int_{D(t)} h(z)\,dx\,dy = 4B(t)\int\int_{D(t)} h(z)\,dx\,dy, \tag{10}$$

where $h(z)$ is any single-valued analytic function in $D(t)$ that is integrable over $D(t)$ (*in the sense of area measure*).

Proof. Using the complex form of Green's theorem [1],

$$\begin{aligned}\frac{d}{dt}\int\int_{D(t)} h(z)\,dx\,dy &= \frac{d}{dt}\frac{1}{2i}\oint_{\partial D(t)} h(z)\bar{z}\,dz \\ &= \frac{1}{2i}\oint_{\partial D(t)} h'(z)z_t\bar{z}dz + h(z)\bar{z}_t dz + h(z)\bar{z}\,dz_t \\ &= \frac{1}{2i}\oint_{\partial D(t)} h(z)\,(\bar{z}_t dz - z_t d\bar{z}),\end{aligned} \tag{11}$$

where the last line follows by integration by parts on the last term in the penultimate line. But the kinematic condition can be written

$$\mathrm{Im}[(z_t - 2\phi_{\bar{z}})\bar{z}_s] = 0, \qquad \text{on } \partial D(t), \tag{12}$$

where s is the local arclength parameter around $\partial D(t)$, or equivalently, as

$$\bar{z}_t dz - z_t d\bar{z} = 2\phi_z dz - 2\phi_{\bar{z}} d\bar{z}, \tag{13}$$

which can be subtituted into (11) to yield

$$\frac{d}{dt}\int\int_{D(t)} h(z)\,dx\,dy = \frac{1}{2i}\oint_{\partial D(t)} h(z)\,(2\phi_z dz - 2\phi_{\bar{z}} d\bar{z}). \tag{14}$$

But ϕ is constant on each part of $\partial D(t)$, which implies

$$d\phi = \phi_z dz + \phi_{\bar{z}} d\bar{z} = 0, \qquad \text{on} \quad \partial D(t). \tag{15}$$

Using this in (14) yields

$$\frac{d}{dt}\int\int_{D(t)} h(z)\,dx\,dy = \frac{1}{2i}\oint_{\partial D(t)} 4h(z)\phi_z\,dz. \tag{16}$$

However, everywhere in the multiply connected $D(t)$, ϕ satisfies

$$\phi_{\bar{z}z} = B(t), \tag{17}$$

so that integration with respect to $\bar{z}$ implies that

$$\phi_z = B(t)\bar{z} + g(z,t), \tag{18}$$

where, by standard results in harmonic analysis [16], it is known that $g(z,t)$ is both analytic and single-valued in the multiply connected $D(t)$. Therefore,

$$\frac{d}{dt}\int\int_{D(t)} h(z)\,dx\,dy = \frac{1}{2i}\oint_{\partial D(t)} 4h(z)(B(t)\bar{z} + g(z,t))\,dz$$
$$= \frac{1}{2i}\oint_{\partial D(t)} 4h(z)B(t)\bar{z}\,dz, \tag{19}$$

using Cauchy's theorem and the fact that the combination $h(z)g(z,t)$ is a single-valued analytic function in $D(t)$. The result follows by a final application of Green's theorem. □

Theorem 2.1 is closely related to results involving the Cauchy transforms of simply connected domains derived by Entov et al. [6] in the context of different but related Hele-Shaw problems and by Shelley et al. [18] in the context of the squeeze flow problem. The theorem above extends these earlier results to multiply connected domains and is stated in a form suited to the analysis involving quadrature identities that follows.

Theorem 2.1 holds regardless of the values of the time-dependent pressures $p_i(t)$ inside the enclosed bubbles. It will be seen later how the values of $p_i(t)$ enter the analysis to affect the dynamical evolution.

3. Quadrature Domains

The simplest example of a quadrature domain [15] is a circular disc. For a disc D of radius r centred at the origin, the *mean value formula* [1] states that

$$\int\int_D h(z)\,dx\,dy = \pi r^2 h(0), \tag{20}$$

where $h(z)$ is an arbitrary function analytic in the disc and integrable over it. (20) shows that the integration of $h(z)$ over the two-dimensional support of the disc can be reduced to the sum of weighted values of $h(z)$ over a finite point set (i.e., just the origin in the case of the circular disc).

As a generalization of this case, a domain D is called a *quadrature domain* if the following *quadrature identity* holds for all $h(z)$ analytic, integrable functions in D:

$$\int\int_D h(z)\,dx\,dy = \sum_{k=1}^{m}\sum_{j=0}^{n_k-1} c_{kj}h^{(j)}(z_k), \tag{21}$$

for some set of coefficients $\{c_{kj}\}$ and some point set $\{z_k\}$. Here $h^{(j)}(z)$ denotes the j-th derivative of $h(z)$. The set of complex numbers $\{c_{kj}\}$ and $\{z_k\}$ is called the *quadrature data* of D.

As an example, Figure 1 shows a configuration in which four discs of unit radius are just touching. The centers of the discs are at $\pm\sqrt{3}$ and at $\pm i$, and each has radius $r = 1$. This resulting (open) domain is disconnected and because integration over such

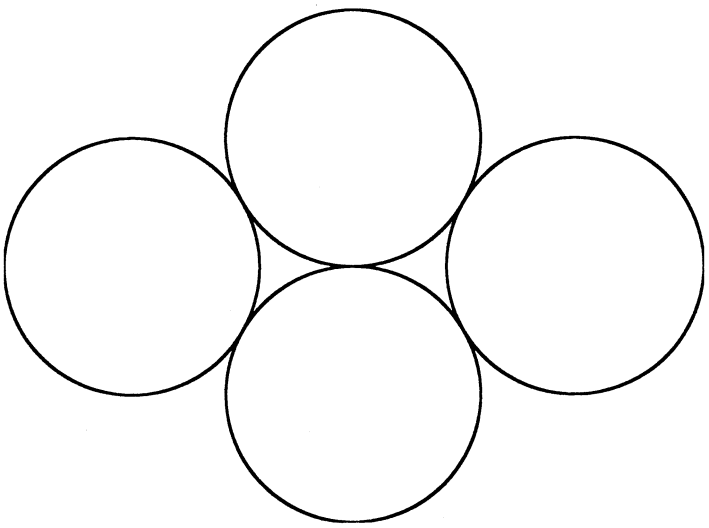

Fig. 1. Initial domain of four equal touching circles of unit radius.

a domain is additive, the mean value formula (20) can be used to deduce that it is a quadrature domain with associated quadrature identity

$$\int\int_D h(z)\,dx\,dy = \pi h(\sqrt{3}) + \pi h(-\sqrt{3}) + \pi h(i) + \pi h(-i). \tag{22}$$

This corresponds to (21) with quadrature data given by

$$\begin{aligned} m = 4, \qquad z_1 = \sqrt{3}, \qquad z_2 = -\sqrt{3}, \qquad z_3 = i, \qquad z_4 = -i, \\ c_{k0} = \pi, \qquad n_k = 1 \qquad (k = 1 \ldots 4). \end{aligned} \tag{23}$$

The objective of this paper is first to show how to produce initial multiply-connected fluid domains by *continuing* an initially disconnected domain of touching discs (such as that in Fig. 1) and then to determine the evolution of such initial multiply-connected fluid blobs under the dynamics of the squeeze flow problem. From Theorem 2.1, the dynamics of this free boundary problem is such that, if the quadrature identity of the initial multiply-connected domain $D(0)$ is

$$\int\int_{D(0)} h(z)\,dx\,dy = \pi r_0^2 h(\sqrt{3}) + \pi r_0^2 h(-\sqrt{3}) + \pi r_0^2 h(i) + \pi r_0^2 h(-i), \tag{24}$$

for some $r_0 > 1$ (note that the case $r_0 = 1$ retrieves the quadrature identity (22) relevant to the disconnected domain of touching open discs), then at later times $t > 0$, the fluid domain $D(t)$ remains a quadrature domain with quadrature identity

$$\begin{aligned} \int\int_{D(t)} h(z)\,dx\,dy \;=\; & \pi r(t)^2 h(\sqrt{3}) + \pi r(t)^2 h(-\sqrt{3}) \\ & + \pi r(t)^2 h(i) + \pi r(t)^2 h(-i), \end{aligned} \tag{25}$$

where

$$r(t)^2 = r_0^2 \exp\left(\int_0^t 4B(t')\,dt'\right). \tag{26}$$

The fact that the dynamics of squeeze flow preserves quadrature domains forms the key result on which the analysis of this paper is based.

4. Algebraic curves

It is known [2] that, if D is a quadrature domain satisfying some identity (21), then its boundary ∂D is part of an *algebraic curve* given, to within a finite set of *special points* V_0, by

$$\partial D = \{z \in \mathbb{C} | \mathcal{P}(z, \bar{z}) = 0\} \backslash V_0, \tag{27}$$

where

$$\mathcal{P}(z, w) = \sum_{k,j=0}^{n} a_{kj} z^k w^j, \tag{28}$$

where $n = \sum_{k=1}^{m} n_k$ is referred to as the *order* of the quadrature identity, and where the coefficients $\{a_{kj}\}$ satisfy the hermitian property

$$\bar{a}_{jk} = a_{kj}. \tag{29}$$

The finite set of points V_0 will be important for our methods and will be discussed in more detail later. The matrix of coefficients $\{a_{kj}\}$ will henceforth be referred to as the matrix $\mathbf{A}$, i.e.,

$$[\mathbf{A}]_{kj} = a_{kj}, \qquad k,\ j = 0 \ldots n. \tag{30}$$

For a quadrature identity of order n, $\mathbf{A}$ will be an $(n+1)$-by-$(n+1)$ matrix. An alternative way of writing (28) is in the form

$$\mathcal{P}(z, w) = \sum_{j=0}^{n} w^j P_j(z), \tag{31}$$

where each $P_j(z)$ is a polynomial of degree at most n.

There is a normalization degree of freedom in the specification of $\mathcal{P}(z, \bar{z})$. Without loss of generality, we set $a_{nn} = 1$.

It is natural to expect there must be some connection between the quadrature data $\{c_{kj}\}$, $\{z_k\}$ and the set of coefficients $\{a_{kj}\}$ defining the associated algebraic curve. Indeed, there is a *partial* connection embodied in the following theorem of Gustafsson [7]:

Theorem 4.1. *For a quadrature domain satisfying the quadrature identity* (21) *of order* n*, the identity*

$$\frac{1}{\pi} \sum_{k=1}^{m} \sum_{j=0}^{n_k - 1} \frac{j! c_{kj}}{(z - z_k)^{j+1}} \equiv a_{nn-1} - \frac{P_{n-1}(z)}{P_n(z)}, \tag{32}$$

where

$$P_{n-1}(z) = a_{n,n-1}z^n + a_{n-1,n-1}z^{n-1} + \cdots + a_{0,n-1}, \tag{33}$$

$$P_n(z) = z^n + a_{n-1,n}z^{n-1} + \cdots + a_{0,n}, \tag{34}$$

sets up a one-to-one correspondence between the set of coefficients $\{c_{kj},\ z_k\}$ *and the last two columns* (*and rows*) *of the coefficient matrix* $\mathbf{A}$.

It is important to realize that this connection between the coefficients is only partial and that, for general n, there is a disparity between the amount of quadrature data $\{c_{kj}\}$, $\{z_k\}$ and the elements of the matrix $\mathbf{A}$. However, Theorem 4.1 shows that there is an upper bound for the degree of this disparity, specifically, the first $(n-1)$ columns (or, equivalently, rows) of the hermitian matrix $\mathbf{A}$ are not explicitly determined by knowledge of the quadrature data. As emphasized by Gustafsson [7], it is in general a difficult matter to determine the full set of coefficients $\{a_{kj}\}$ (defining the algebraic curve associated with a quadrature domain) purely from knowledge of the quadrature data in (21). In this paper, we address precisely this issue.

5. Special Points of Quadrature Domains

Gustafsson [8] has discussed how points of contact of disconnected circular domains leave so-called "special points" z_s inside the domain as the domain changes such as to become connected. Such special points are defined as being *isolated* solutions of

$$\mathcal{P}(z_s, \bar{z}_s) = 0, \tag{35}$$

and do not, in general, constitute part of the continuous boundary of the quadrature domain. These points constitute the finite set V_0 referred to in Section 4. Moreover, at such points, it is known that the following holds:

$$\frac{\partial \mathcal{P}(z_s, \bar{z}_s)}{\partial z} = \frac{\partial \mathcal{P}(z_s, \bar{z}_s)}{\partial \bar{z}} = 0. \tag{36}$$

We refer the reader to Gustafsson [8] for a detailed discussion of these special points. The study of such points seems to originate from the work of Shapiro [17].

For quadrature identities possessing certain geometrical symmetries, it is natural to seek associated quadrature domains sharing the same symmetries. In certain cases, it is possible to exploit these symmetries as well as properties concerning the special points of the domain (as established in [8]) to deduce important information about the "unknown" data of the matrix $\mathbf{A}$. In very special cases, these considerations are enough to determine all such data (cf: Section 6), however, in the general case, only partial additional information is obtained (cf: Section 7). We will illustrate these two possible cases by example and, for practical purposes of constructing multiply-connected quadrature domains, show how we propose to overcome the "information deficit" when symmetry considerations and information regarding special points is not sufficient to identify all the unknown parameters of the algebraic curve.

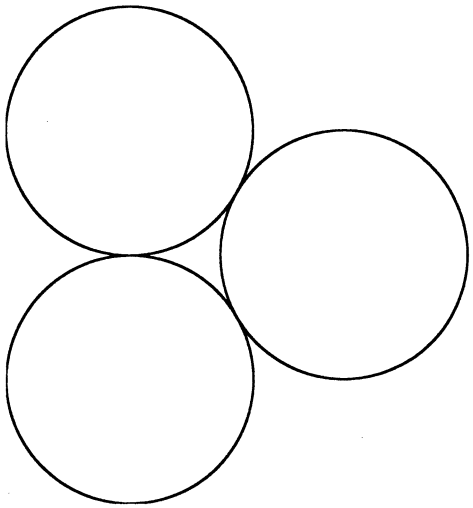

Fig. 2. Initial domain of three equal touchingcircles of unit radius.

6. A Doubly-Connected Fluid Domain

To illustrate the general method, we first present details of the construction of a doubly-connected quadrature domain. The following presentation is based in essence on that given in [7] but differs in detail and emphasis. This example is illustrative but, unfortunately, rather special. This is because, as will be seen, it is possible in this example to use information on the special points of the quadrature domain to obtain *complete* information on the unknown parameters describing the algebraic curve.

In Figure 2, three equal unit discs are placed in an annular configuration about the origin. By the mean value formula (20), this domain is a quadrature domain D satisfying the quadrature identity:

$$\int\int_D h(z)\,dx\,dy = \pi h(z_1) + \pi h(z_2) + \pi h(z_3), \tag{37}$$

where

$$z_1 = \frac{2}{\sqrt{3}}; \qquad z_2 = \frac{2}{\sqrt{3}} e^{\frac{2i\pi}{3}}; \qquad z_3 = \frac{2}{\sqrt{3}} e^{\frac{4i\pi}{3}}. \tag{38}$$

(37) is a quadrature identity of order 3. It turns out that the corresponding algebraic curve is also easy to find because the (open) domain is disconnected and corresponds to a situation in which the polynomial $\mathcal{P}$ is reducible. Indeed, it is straightforward to deduce that

$$\mathcal{P}(z,\bar{z}) = (|z-z_1|^2 - 1)(|z-z_2|^2 - 1)(|z-z_3|^2 - 1) = 0, \tag{39}$$

with z_1, z_2, and z_3 as in (38). This simplifies to

$$\mathcal{P}(z,\bar{z}) = z^3\bar{z}^3 - \frac{8}{3\sqrt{3}}(z^3 + \bar{z}^3) - 3z^2\bar{z}^2 - z\bar{z} + \frac{1}{27} = 0. \tag{40}$$

The corresponding matrix $\mathbf{A}$ is

$$\mathbf{A} = \begin{pmatrix} \frac{1}{27} & 0 & 0 & -\frac{8}{3\sqrt{3}} \\ 0 & -1 & 0 & 0 \\ 0 & 0 & -3 & 0 \\ -\frac{8}{3\sqrt{3}} & 0 & 0 & 1 \end{pmatrix}. \tag{41}$$

Now consider the quadrature identity

$$\int\int_D h(z)\,dx\,dy = \pi r^2 h(z_1) + \pi r^2 h(z_2) + \pi r^2 h(z_3), \tag{42}$$

where r is just greater than unity. Note that all the coefficients of the different $h(z_j)$ have changed symmetrically. This will also be true under the dynamics of the squeeze flow problem.

By Theorem 4.1, the matrix corresponding to the time-evolving quadrature identity is given by

$$\mathbf{A} = \begin{pmatrix} f & 0 & 0 & -\frac{8}{3\sqrt{3}} \\ 0 & e & 0 & 0 \\ 0 & 0 & -3r^2 & 0 \\ -\frac{8}{3\sqrt{3}} & 0 & 0 & 1 \end{pmatrix}, \tag{43}$$

where we have assumed a three-fold rotational symmetry so that all off-diagonal elements are zero except for those shown in (43). It is important to realize that two of the entries, e and f, are not determined explicitly by the quadrature data. It remains to find this parameter pair (e, f). Note that comparison of (41) and (43) shows that the initial domain in Figure 2 is given by the parameter values

$$r = 1, \qquad e = -1, \qquad f = \frac{1}{27}. \tag{44}$$

By the symmetry of the configuration, we expect to find special points of the time-evolving quadrature domains on the rays

$$\arg[z] = \frac{\pi + 2\pi l}{3}, \qquad l = 0,\ 1,\ 2. \tag{45}$$

Note that the initial points of contact of the touching circles lie on these rays. For $r > 1$, we expect that the disconnected domain in Figure 1 will become connected and that these points of contact will generate special points in the *interior* of the resulting connected domain. For a detailed explanation of this phenomenon, we refer the reader to Gustafsson [8].

Define a function $p(s)$ as follows:

$$p(s) = \mathcal{P}(se^{\frac{i\pi}{3}}, se^{-\frac{i\pi}{3}}), \tag{46}$$

where s is some real parameter. If s is to correspond to the distance of this expected special point from the origin, then

$$\begin{aligned} p(s) &= 0, \\ p'(s) &= 0. \end{aligned} \tag{47}$$

These two equations result from (35) and (36), which are necessary conditions at a special point.

For a doubly connected domain, we expect one specifiable degree of freedom associated with the hole in the domain. Intuitively it is convenient to think of this degree of freedom as associated with specifying the area of the hole. This point is discussed in some detail (with respect to domains of arbitrary connectivity) in Theorems 11 and 12 of Gustafsson [7]. For present purposes, we choose to fix the parameter s. With s fixed, we expect to find a corresponding uniquely defined domain. It will be seen later how this degree of freedom is associated with the (as yet, unused) information regarding the externally-specified pressures $p_i(t)$ of the air inside the enclosed air holes.

Once s is set, two equations for the unknown pair $(e,\ f)$ are provided by (47). Indeed, these equations are linear in $(e,\ f)$ once s and r are specified, and some manipulation gives the following explicit results:

$$\begin{aligned} e &= 6r^2s^2 - \frac{8}{\sqrt{3}}s - 3s^4, \\ f &= 2s^6 - 3r^2s^4 + \frac{8}{3\sqrt{3}}s^3. \end{aligned} \tag{48}$$

To verify this, it is instructive to construct a conformal mapping from the annulus $\rho < |\zeta| < 1$ in a parametric ζ-plane to this class of doubly connected domains. Gustafsson [8] also mentions this fact and that the corresponding conformal map must be an elliptic function (from a rectangular parametric region). While a general representation of such a map is written down in [8] in terms of Weierstrass-$\mathcal{P}$ functions, no explicit examples are presented. Here, for illustrative purposes, we will explicitly construct such a map, but we choose to do so in a more convenient way using a special function $Q_3(\zeta;\ \rho)$ defined in terms of the following infinite product:

$$Q_3(\zeta;\ \rho) = (1-\zeta^3)\prod_{n=1}^{\infty}(1-\rho^{6n}\zeta^3)(1-\rho^{6n}\zeta^{-3}). \tag{49}$$

The required conformal map is then given as

$$z(\zeta) = R\zeta\,\frac{Q_3(\zeta\rho^{2/3}a^{-1};\ \rho)}{Q_3(\zeta a^{-1};\ \rho)}, \tag{50}$$

where R, a, and ρ are real parameters with $0 < \rho < 1$ and $1 < a < \rho^{-1}$. To verify that this is the case, first observe that $Q_3(\zeta;\ \rho)$ satisfies

$$Q_3(\rho^2\zeta;\ \rho) = -\frac{1}{\zeta^3}Q_3(\zeta;\ \rho) = Q_3(\zeta^{-1};\ \rho), \tag{51}$$

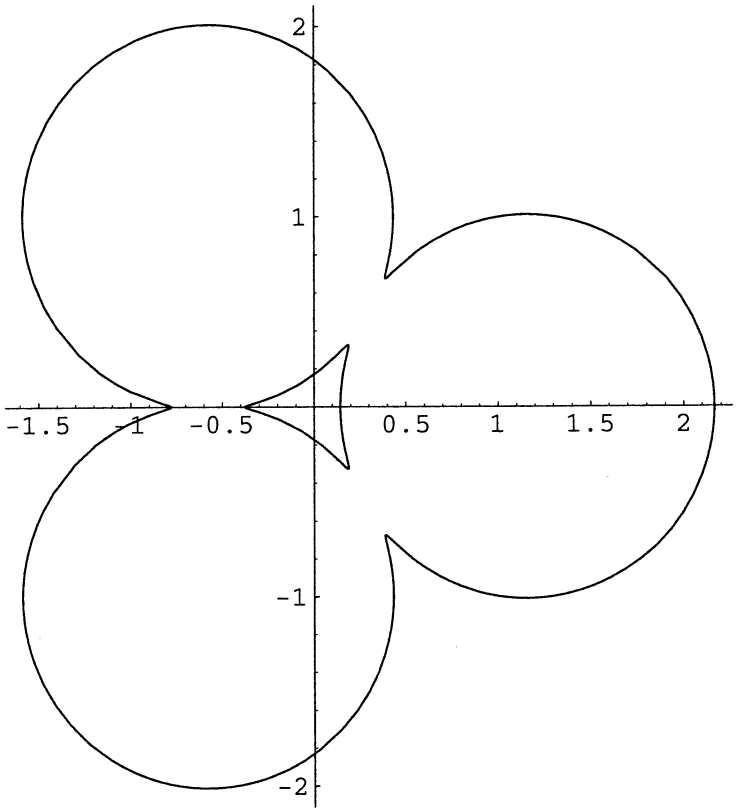

Fig. 3. An example of a doubly connected domain drawn using both the conformal map and the corresponding algebraic curve.

which can be used to verify that $z(\zeta)$ satisfies the functional equation

$$z(\rho^2\zeta) = z(\zeta), \tag{52}$$

which can, in turn, be used to verify that this domain is a quadrature domain satisfying the identity (42). The function (50) is a *loxodromic function* [20] [14] and is related to an elliptic function by a simple exponential transformation.

The two intersection points of the boundary of the domain with the positive real axis should correspond to points $z(\rho)$ and $z(1)$, while it is necessary that $z(a^{-1}) = z_1$ where z_1 is defined in (38). Figure 3 shows a typical doubly-connected quadrature domain constructed using the algebraic curve method just described, and the numerical values of $z(\rho)$, $z(1)$, and $z(a^{-1})$ are determined from this graph. This provides three nonlinear equations for R, a, and ρ, which are solved using Newton's method. The image of the annulus $\rho < |\zeta| < 1$ under the conformal map (50) with the resulting parameter values is also plotted in Figure 3 and corresponds exactly to the algebraic curve.

This example illustrates the relationship between the proposed new solution method using algebraic curves and the traditional approach to such problems based on constructing a uniformization map (or conformal map). We now illustrate our methods in the case of fluid domains of connectivity greater than two where uniformization maps are much more challenging to construct. The new method obviates the need to construct such uniformization maps and pertains to fluid domains of any finite connectivity.

7. Evolution of a Triply-Connected Fluid Blob

As a first example, we return to the configuration in Figure 1. It has already been deduced that, under the dynamics of squeeze flow, an initial domain satisfying the quadrature identity (24) for some $r_0 > 1$ satisfies the identity (25) under evolution with $r(t)$ given by (26). (25) is a quadrature identity of order 4. Under the dynamics of squeeze flow, the weights c_{k0} of each of the $h(z_k)$ in (22) change equally in time (i.e., they are all equal to $r(t)^2$ at time t). The configuration in Figure 1 has reflectional symmetries about both x and y axes. Because of the equal change in the weights $c_{k0}(t)$ under evolution, we expect to be able to find a class of evolving domains possessing these same reflectional symmetries. In what follows, the explicit time dependence of the parameters is omitted for convenience.

In this case, the domain has sufficient symmetries that the special points of the domain can be exploited in the determination of the algebraic curve. Relative to the point $(\frac{1}{\sqrt{3}}, 0)$ on the real axis, the three circles farthest to the right in Figure 1 share a three-fold rotational symmetry. Also, relative to this point, the three points of contact are symmetrical and occur on rays

$$\arg\left[z - \frac{1}{\sqrt{3}}\right] = \frac{\pi + 2l\pi}{3}, \qquad l = 0,\ 1,\ 2. \tag{53}$$

The same is true of the three leftmost circles (in Figure 1) relative to the point $(-\frac{1}{\sqrt{3}}, 0)$; i.e., the points of contact are symmetric and located on the rays

$$\arg\left[z + \frac{1}{\sqrt{3}}\right] = \frac{2l\pi}{3}, \qquad l = 0,\ 1,\ 2. \tag{54}$$

In the generalized quadrature identity (25) under consideration, all coefficients are changed by the same amount. It is therefore natural to seek quadrature domains satisfying (25) where, for $r > 1$, the special points remain on the rays (53) and (54) relative to the two points $(\frac{1}{\sqrt{3}}, 0)$ and $(-\frac{1}{\sqrt{3}}, 0)$, respectively. In addition, in Figure 1 there is also a point of contact between circles at the origin $(0, 0)$. The reflectional symmetries of the quadrature domain force one of the special points, for $r > 1$, to be at $(0, 0)$.

Using Theorem 4.1, along with the assumed reflectional symmetry properties of the domain, the matrix $\mathbf{A}$ associated with the quadrature identity (25) is deduced to be

$$\mathbf{A} = \begin{pmatrix} k & 0 & g & 0 & -3 \\ 0 & f & 0 & 4r^2 & 0 \\ g & 0 & e & 0 & -2 \\ 0 & 4r^2 & 0 & -4r^2 & 0 \\ -3 & 0 & -2 & 0 & 1 \end{pmatrix}, \tag{55}$$

where the parameters $(e,\ f, g, k)$ remain to be determined. The parameter set corresponding to the initial disconnected domain of touching discs shown in Figure 1 is

$$r = 1, \qquad e = 2, \qquad f = -8, \qquad g = 1. \tag{56}$$

These values can easily be determined by writing down the equation for $\mathcal{P}(z, \bar{z})$ for this case (i.e., the analogue of (40)).

The fact that the origin is a special point implies that

$$k = 0. \tag{57}$$

Now define a function $\mathcal{Q}(z, \bar{z})$ as follows:

$$\mathcal{Q}(z, \bar{z}) \equiv \mathcal{P}\left(\frac{1}{\sqrt{3}} + z, \frac{1}{\sqrt{3}} + \bar{z}\right), \tag{58}$$

a transformation that amounts to a change of origin from $(0, 0)$ to $(\frac{1}{\sqrt{3}}, 0)$. Following the procedure used in Section 6, define a function $q(s)$ as

$$q(s) = Q(se^{\frac{i\pi}{3}}, se^{-\frac{i\pi}{3}}). \tag{59}$$

In order that the real parameter s represents the distance of the special point from the point $(\frac{1}{\sqrt{3}}, 0)$, we must have

$$\begin{aligned} q(s) &= 0, \\ q'(s) &= 0. \end{aligned} \tag{60}$$

These follow from conditions (35) and (36). By the reflectional symmetries of the domain, condition (60) will immediately ensure that there are three other symmetrically-disposed special points in the domain so that we have now exhausted all possible information arising from the expected special points of the domain. We expect a single degree of freedom (for any given value of r) in the determination of the quadrature domain—a freedom associated with specifying the area of the enclosed bubbles (by symmetry, the area of the two bubbles must be the same). It will be supposed that specifying s corresponds to fixing this degree of freedom. With r and s given, there remain three undetermined parameters $(e,\ f, g)$ and only two equations (60).

An additional equation is introduced by exploiting the quadrature identity. Putting $h(z) = 1$ in (25), we obtain the nonlinear equation

$$\mathcal{F}(e,\ f, g) = 0, \tag{61}$$

where

$$\mathcal{F}(e,\ f, g) \equiv \frac{1}{2i}\oint_{\partial D} \bar{z}dz - 4\pi r^2. \tag{62}$$

(61) is simply the area relation. Note that the dependence of $\mathcal{F}$ on the parameter set $(e,\ f, g)$ is rather subtle: It derives purely from the fact that the integration is a line integral around the algebraic curve ∂D parametrized by $(e,\ f, g)$. Not all such algebraic curves are the boundaries of a quadrature domain: Indeed, it is expected that only one such choice of $(e,\ f, g)$ will yield the boundary of a quadrature domain, and these special values will be given by the simultaneous solution of the three equations (60) and (61).

Equations (60) are linear in $(e,\ f, g)$ so that, given any r, s, and g, they are easily solved to find $(e,\ f)$ in terms of r, s, and the unknown g. These expressions are then used in (61) so that it becomes a single real nonlinear equation for g.

This nonlinear equation is solved using a numerical scheme based on Newton's method. For given $r > 1$ and s, an initial guess is made for g (for values of r just above 1, the value $g = 1$ derived from the initial disconnected configuration of touching discs can be used). An exact formula for the algebraic curve D is then known. Given this formula, $\mathcal{N}$ points, equally spaced in arclength around each closed contour, are determined. This resampling of points is easily found because exact formulae for the tangent and curvature at each point are available from the equation $\mathcal{P}(z, \bar{z}; t) = 0$. Moreover, symmetry implies that it is enough to compute points in the first quadrant. In the following calculation, 120 points are taken on each contour in the first quadrant. The line integral in (61) is then computed using a trapezoidal rule that gives super-algebraic convergence for smooth periodic functions on smooth domains (which is the case here). We then iterate on values of g until (61) is satisfied to acceptable accuracy.

A note on the numerical implementation. At present, the general method described above has been implemented in its most basic form, but is nevertheless found to give excellent accuracy even for boundaries with points of high curvature (see later calculations). More sophisticated numerical manifestations of this scheme can be envisaged; in particular, in the event that the dynamics leads to the development of cusps, it is clearly advisable to concentrate points in the vicinity of the cusp. Such numerical enhancements will not be discussed here.

An important check on the quadrature domains is to make arbitrary choices of single-valued analytic functions $h(z)$ and to numerically compute the line integral

$$\frac{1}{2i}\oint_{\partial D(t)} h(z)\bar{z}\, dz. \tag{63}$$

The numerical result can then be compared to that given by the quadrature identity.

7.1. Properties of the Quadrature Domains

Before computing their evolution under the squeeze flow dynamics, it is first instructive to survey some of the general properties of the quadrature domains for various choices of r and s. Figure 4 shows plots of different quadrature domains for fixed $r = 1.01$ and the three different values $s = 0.67, 0.59, 0.49$. The special points are also marked on these diagrams. When $s = 0.67$ (the first diagram in Figure 4), four of the special points have

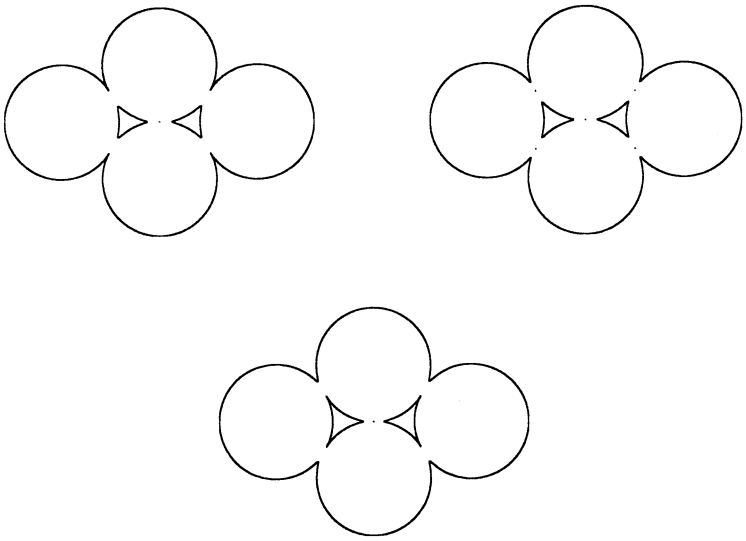

Fig. 4. Triply-connected quadrature domain: $r = 1.01$, $s = 0.67$ (upper left), $s = 0.59$ (upper right), $s = 0.49$ (lower).

drawn close to the continuous outer boundary of the domain, and it is clear that a cusp is forming on this outer boundary. On the other hand, when s is at the lower end of its admissible range, $s = 0.49$, these four special points have drawn close to a point on one of the enclosed boundaries of the domain, and a cusp develops. The middle diagram of Figure 4 gives a typical intermediate case in which all special points are clearly visible. The range $s \in [0.49, 0.67]$ roughly represents the range of existence of solutions for this value of r.

In Figure 5, graphs of (e, f, g) (giving triply-connected quadrature domains) are plotted against s. While the values are shown only for a discrete set of s-values, it is clear that these solutions lie on continuous, smooth curves.

To verify that this behaviour is generic, Figure 6 shows quadrature domains for (fixed) $r = 1.02$ and s values $s = 0.68, 0.57, 0.47$. The interval $s \in [0.47, 0.70]$ roughly represents the total range of existence of domains for this value of r. The first and last diagrams in Figures 6 show cases in which the special points draw close to the outer and inner boundaries respectively, with cusps forming on those boundaries as a result. The middle diagram shows an intermediate case. Such phenomena are consistent with the scenarios described by Gustafsson [8]. In Figure 7, the solutions for (e, f, g) yielding triply-connected quadrature domains are plotted at a discrete set of s values.

Earlier it was stated that the freedom to specify s amounts to specifying the area of the enclosed holes. Figures 8 and 9 show graphs of the total area of the two enclosed holes as functions of the parameter s (for values $r = 1.01$ and $r = 1.02$ respectively) throughout the range of s for which quadrature domains exist. These graphs confirm that this enclosed area is, in fact, a monotonic function of s so that specifying s corresponds to a unique choice of the area of the holes. In applications, the area of the holes will be determined by the relevant physical conditions imposed inside the holes. One possibility is that vents are placed in these holes so that the amount of enclosed air is directly

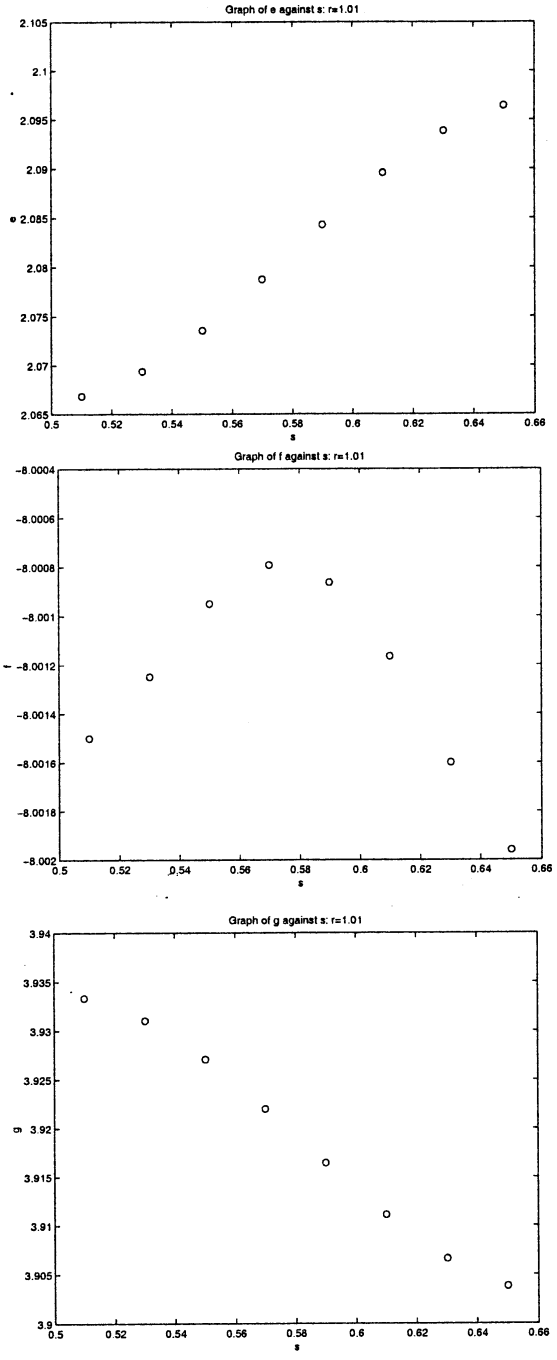

Fig. 5. From top to bottom, graphs of $(e,\ f, g)$ against s for $r = 1.01$.

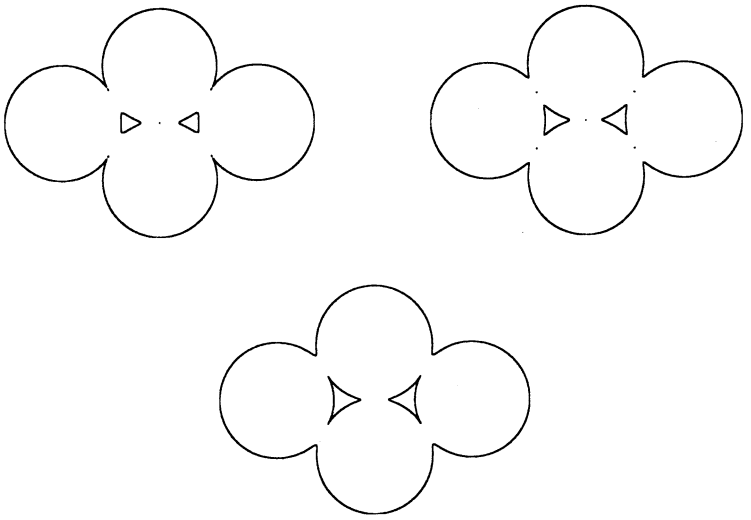

Fig. 6. Triply-connected quadrature domain: $r = 1.02$, $s = 0.68$ (upper left), $s = 0.57$ (upper right), $s = 0.47$ (lower).

controlled. Another scenario is to directly specify the pressure of the air inside the holes (i.e., the pressures $p_i(t)$). In the present context of squeeze flow in a Hele-Shaw cell, the most natural assumption is that the holes are closed (there are no vents) and contain incompressible air, so that the area of each hole remains constant under evolution. This will be the assumption used in the evolutionary calculations that follow.

The numerical method described above converges to the relevant g value for a *given* r and s. In the squeeze flow problem, s is not arbitrarily specified but is determined by the condition of constancy of area of the enclosed holes. In this case, the above Newton iteration is simply extended to an iteration on the values of *both* parameters g and s so that equation (61) *and* the equation constraining the area of the enclosed bubbles are satisfied.

7.2. Evolution Under Squeeze-Flow Dynamics

To illustrate the use of algebraic curves in plotting explicit solutions, we now suppose that the cell is squeezed in such a way that $r(t)$ evolves according to

$$r(t) = r(0)e^t. \tag{64}$$

The area of each air hole is assumed to be fixed in time.

As an example, the following algebraic curve data bounding an initial quadrature domain is chosen:

$$r = 1.028; \qquad e = 2.232; \qquad f = -8.011; \qquad g = 3.778. \tag{65}$$

The area of each of the enclosed air holes is 0.073. This initial domain, shown in Figure 10, corresponds to a fluid domain with four near-cusps on the outer boundary. The subsequent evolution at three successive times is also shown in Figure 10 and reveals the formation,

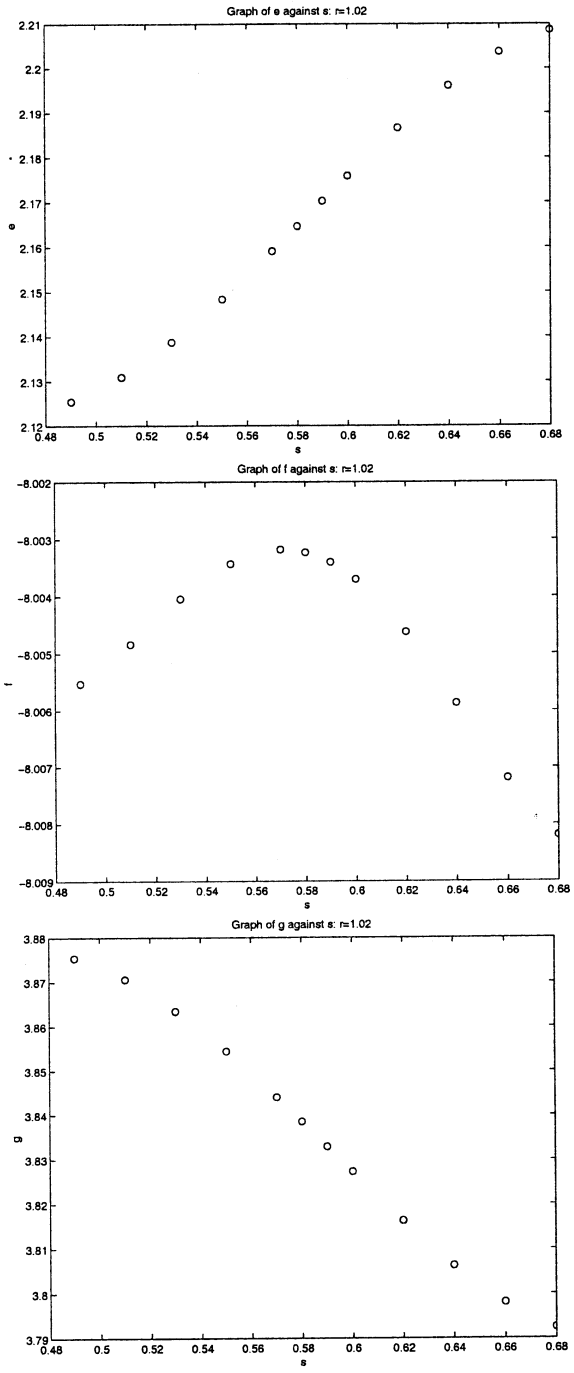

Fig. 7. From top to bottom, graphs of $(e,\ f, g)$ against s for $r = 1.02$.

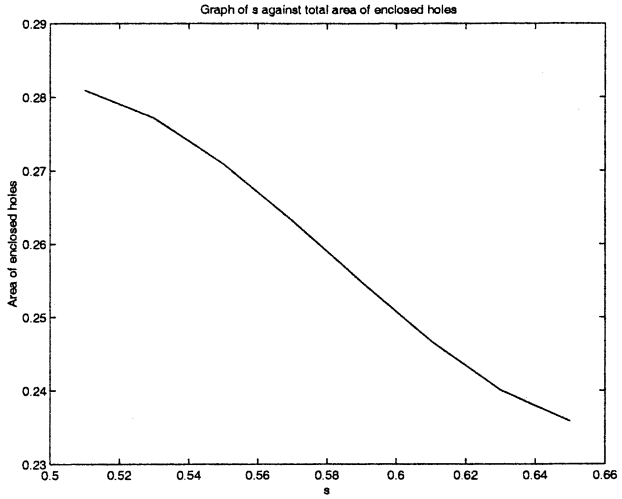

Fig. 8. Graph of total area of enclosed holes against s: $r = 1.01$.

by time $t = 0.0325$, of four points of large curvature, two on each of the boundaries of the two enclosed air holes. Although the numerical calculation was not continued beyond this time (the present implementation of the numerical method is not sophisticated enough to deal reliably with points of extremely high curvature), we suspect the eventual formation of a $\frac{3}{2}$-cusp and subsequent breakdown of the classical solution just after $t = 0.0325$. Note, however, that consistent with the results of Shelley et al. [18], the outer boundary becomes smoother as the plates are squeezed together.

It is important to point out that the use of information regarding the special points of the domain is *not* a necessary component of the method. Here, we have exploited the

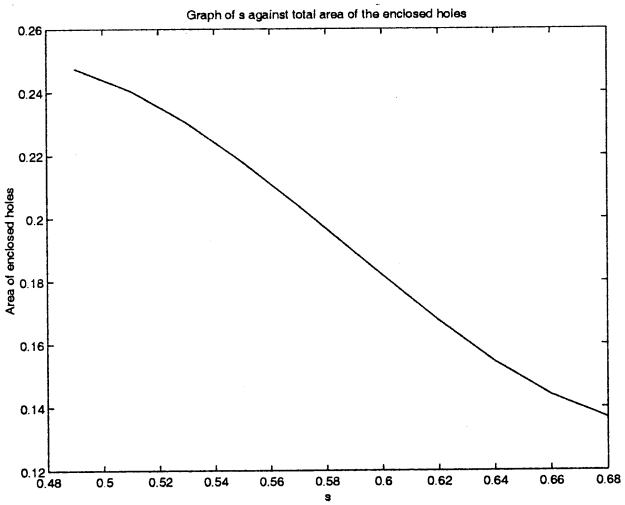

Fig. 9. Graph of total area of enclosed holes against s: $r = 1.02$.

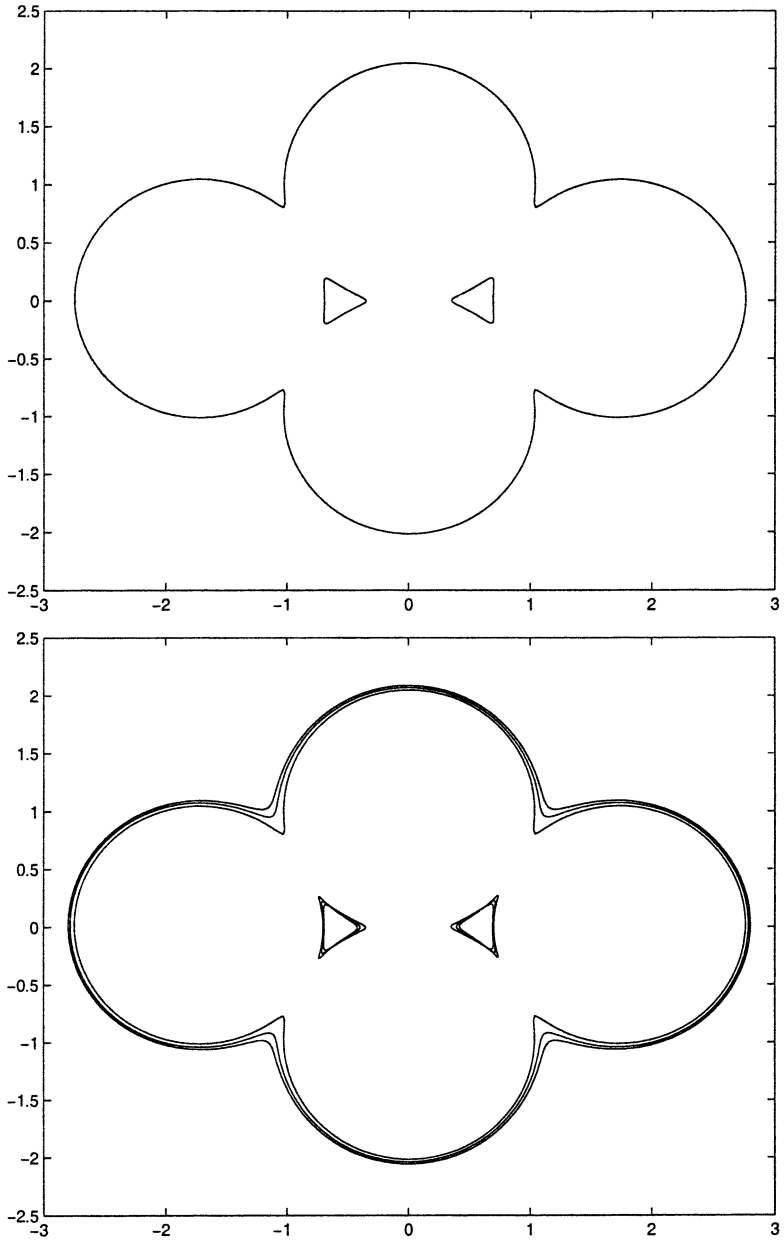

Fig. 10. Upper diagram shows the initial triply-connected domain. Lower diagram shows superposition of the subsequent evolution under squeeze dynamics at times $t = 0.0$, 0.02, and 0.0325.

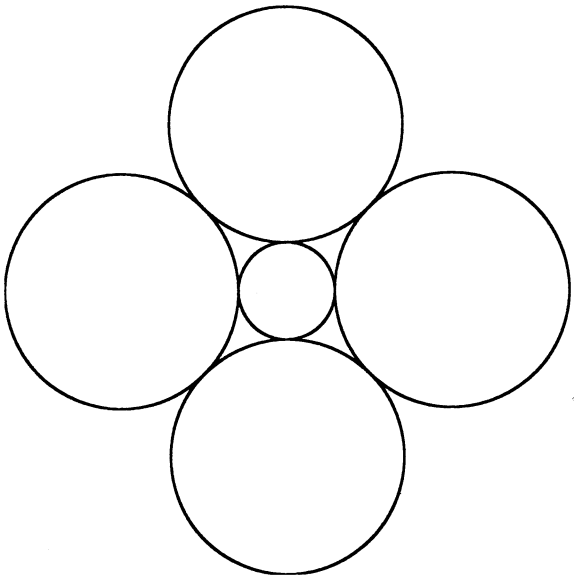

Fig. 11. Initial disconnected domain of five (unequal) touching discs which is continued to construct a quintuply-connected quadrature domain.

special points to reduce the reconstruction of the algebraic curve to the solution of just two real nonlinear equations for g and s. If we did not wish to use the special points, we could alternatively solve three real nonlinear equations directly for $(e,\ f, g)$. The additional equations can be generated by taking different (linearly independent) choices of $h(z)$ in the quadrature identity and using Green's theorem. In the general case (i.e., those with little symmetry), special points are of little help and the latter approach must be used.

8. Evolution of a Quintuply Connected Blob

To illustrate the generality of the approach, the evolution of a quintuply connected fluid blob with four air holes is now calculated. The initial domain is taken to be a continuation of the disconnected domain of touching discs shown in Figure 11 and is constructed in an analogous way to that described in detail in the context of the triply connected example. In this case, the algebraic curve matrix **A** has the form

$$\mathbf{A} = \begin{pmatrix} k & 0 & 0 & 0 & 4p^2 & 0 \\ 0 & g & 0 & 0 & 0 & -4 \\ 0 & 0 & f & 0 & 0 & 0 \\ 0 & 0 & 0 & e & 0 & 0 \\ 4p^2 & 0 & 0 & 0 & -(4r^2 + p^2) & 0 \\ 0 & -4 & 0 & 0 & 0 & 1 \end{pmatrix}, \tag{66}$$

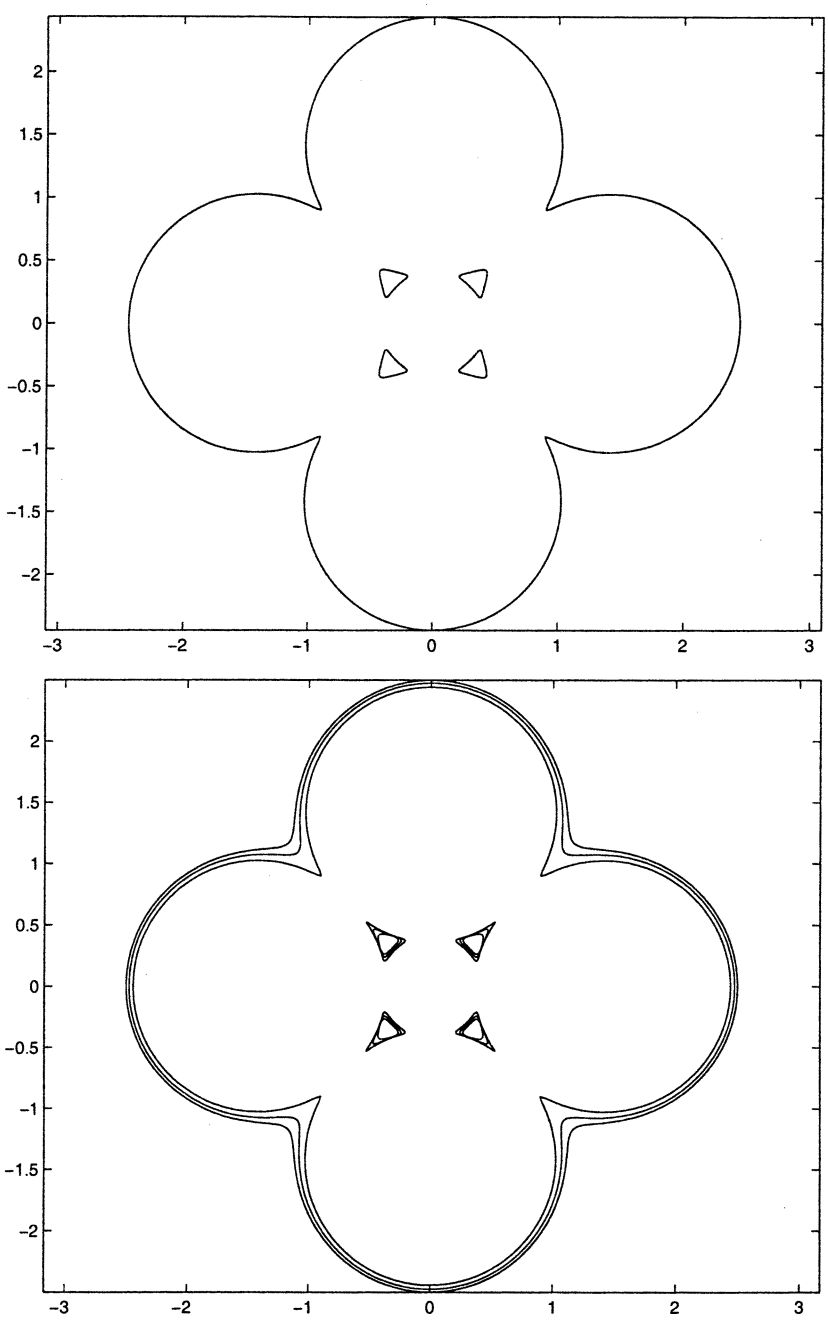

Fig. 12. Upper diagram shows the initial quintuply-connected domain with four enclosed air holes. Lower diagram shows superposition of the subsequent evolution under squeeze dynamics at times $t = 0.0$, 0.025, and 0.0425.

where it will be supposed that the rate of squeezing is such that

$$r(t) = r(0)e^t, \qquad p(t) = p(0)e^t. \tag{67}$$

The area of each of the four enclosed holes is again assumed constant.

The addition of two more holes has no effect on the general method other than a change in the relevant polynomial $\mathcal{P}(z, \bar{z}; t)$ and its associated matrix $\mathbf{A}(t)$. With r and p given explicitly at each instant by (67), there are four real elements of the $\mathbf{A}(t)$, namely $\{e(t),\ f(t), g(t), k(t)\}$, to be determined. This is done using the same methodology described in the context of the triply connected example. It is noted that this class of quintuply connected domains again has sufficient symmetry to enable information on the special points to reduce the number of unknown parameters in the Newton iteration to just two. More details of the construction of such domains can be found in Crowdy [5].

The initial algebraic curve shown in Figure 12 is given by parameters

$$\begin{aligned} r &= 1.029, \qquad p = 0.410, \qquad e = -0.968, \\ f &= -3.555, \qquad g = 1.391, \qquad k = -0.127. \end{aligned} \tag{68}$$

The area of the enclosed air holes remains constant and equal to 0.027.

An initial domain is again chosen with four points of high curvature in the outer boundary and four enclosed air holes with relatively smooth boundaries. Superposed plots of the subsequent domains at times $t = 0.0, 0.025$, and 0.0425 are shown in Figure 12. As the plates of the cell are moved together, the points of high curvature in the outer boundary are smoothed out while the air holes are squeezed in such a way that each develops a single point of increasingly large curvature on its boundary which is a manifestation of the incipient formation of four $\frac{3}{2}$-cusps. With no physical mechanism to regularize this cusp formation, the solution will break down just after $t = 0.0425$.

9. Discussion

This paper has demonstrated that the squeeze flow problem admits exact solutions for a wide class of multiply-connected fluid domains. It has also demonstrated the efficacy of using algebraic curves to explicitly reconstruct the evolving fluid domains in terms of a finite set of time-evolving parameters. In an example of a triply connected domain, the evolution was tracked in terms of four real parameters, $\{r(t), e(t),\ f(t), g(t)\}$ while a quintuply connected domain required calculation of the evolution of just six real parameters $\{r(t),\ p(t), e(t),\ f(t), g(t), k(t)\}$.

An alternative approach would be to construct uniformization maps; Gustafsson [7] has shown that the construction of a conformal map to the triply connected and quintuply connected regions considered here would involve the construction of a class of meromorphic functions on Riemann surfaces of genus 2 and 4 respectively. This might be done by constructing the appropriate automorphic functions on the universal cover of these compact Riemann surfaces (the rational functions and elliptic functions represent examples in the case of genus 0 and 1). Even using this traditional approach, fitting the conformal mapping parameters to the quadrature data involves, in general, finding

the numerical solution to a finite system of nonlinear equations. The use of algebraic curves obviates the need to construct such uniformization maps, and works in the same way regardless of the connectivity of the fluid domain. It too involves no more than the numerical solution of a finite system of nonlinear equations. The conceptual simplicity of the algebraic curve approach only adds to its practical appeal.

Another convenience of our approach concerns changes in topology. If the physical problem entails the shrinking and eventual vanishing of air holes, the method expounded here captures these events automatically—the algebraic curve $\mathcal{P}(x + iy, x - iy) = 0$ simply ceases to possess quite as many solutions for real x and y. Using conformal maps in order to capture the disappearance of an air hole, it would be necessary to alter the topology of the canonical parametric region mapping to the fluid domain and thus, in general, the functional form of the conformal map.

The methods here are relevant to any free boundary problem in which the dynamics preserves quadrature domains or, equivalently, the rational character of the Cauchy transform of the initial domain. Such problems include singularity-driven Hele-Shaw flows [12]. Recently, Crowdy [4] has considered an abstract class of geometry-driven free boundary problems which are such as to preserve the rational character of the Cauchy transform and has shown that the problem of flow in a rotating Hele-Shaw cell [3] and the biharmonic-governed problem of viscous sintering both fall within this class. The methods of domain reconstruction described herein are applicable to such problems.

Acknowledgments

The first author gratefully acknowledges partial financial support from the National Science Foundation (Grant Nos. DMS-9803167 and DMS-9803358) and from the Nuffield Foundation.

References

[1] M. Ablovitz & A. S. Fokas, *Complex variables*, Cambridge University Press, Cambridge (1997).
[2] D. Aharonov & H. Shapiro, Domains on which analytic functions satisfy quadrature identities, *J. Anal. Math.*, **30**, 39–73 (1976).
[3] D. G. Crowdy, Theory of exact solutions for the evolution of a fluid annulus in a rotating Hele-Shaw cell, *Q. Appl. Math.* (to appear).
[4] D. G. Crowdy, On a class of geometry-driven free boundary problems, *SIAM J. Appl. Math.* (to appear).
[5] D. G. Crowdy, On the construction of multiply-connected quadrature domains, *SIAM J. Appl. Math.* (to appear).
[6] V. M. Entov, P. I. Etingof, & D. Ya Kleinbock, On nonlinear interface dynamics in Hele-Shaw flows, *Eur. J. Appl. Math.*, **6**, 399–420, (1995).
[7] B. Gustafsson, Quadrature identities and the Schottky double, *Acta. Appl. Math.*, **1**, 209–240 (1983).

[8] B. Gustafsson, Singular and special points on quadrature domains from an algebraic geometric point of view, *J. Anal. Math.*, **51**, 91–117 (1988).
[9] P. P. Kufarev, The oil contour problem for the circle with any number of wells, *Dokl. Akad. Nauk SSSR*, **75**, 507–510 (1950).
[10] G. A. Jones & D. Singerman, *Complex functions*, Cambridge University Press, Cambridge (1987).
[11] P. Ya. Polubarinova-Kochina, On the motion of the oil contour, *Dokl. Akad. Nauk SSSR*, **47**, 254–257 (1945).
[12] S. Richardson, Some Hele-Shaw flows with time-dependent free boundaries, *J. Fluid Mech.*, **102**, 263–278 (1981).
[13] S. Richardson, Hele-Shaw flows with time-dependent free boundaries in which the fluid occupies a multiply connected region, *Eur. J. Appl. Math.*, **5**, 97–122 (1994).
[14] S. Richardson, Hele-Shaw flows with time-dependent free boundaries involving a concentric annulus, *Phil. Trans. R. Soc. Lond.*, **354**, 2513–2553 (1996).
[15] M. Sakai, Quadrature domains, *Lecture Notes in Mathematics*, **934**, Springer-Verlag, New York (1982).
[16] S. Saks & A. Zygmund, *Analytic functions*, 3rd ed., Elsevier, Amsterdam (1971).
[17] H. S. Shapiro, Unbounded quadrature domains, in *Complex Analysis I, Proceedings, University of Maryland* 1985–86, C. A. Bernstein (ed.), Lecture Notes in Mathematics, **1275**, Springer-Verlag, Berlin (1987), pp. 287–331.
[18] M. J. Shelley, F. R. Tian, & K. Wlodarski, Hele-Shaw flow and pattern formation in a time-dependent gap, *Nonlinearity*, **10**, 1471–1495 (1997).
[19] M. Siegel, S. Tanveer, & W. S. Dai, Singular effects of surface tension in evolving Hele-Shaw cells, *J. Fluid Mech.*, **323**, pp. 201–236 (1996).
[20] G. Valiron, *Cours d'analyse mathematique*: *Theorie des fonctions*, 2nd ed., Masson et Cie, Paris (1940).
[21] A. N. Varchenko & P. I. Etingof, Why the boundary of a round drop becomes a curve of order four, *University Lecture Series*, American Mathematical Society, Providence, RI (1992).